

Active vs passive scalar turbulence

Antonio Celani¹, Massimo Cencini², Andrea Mazzino^{3,4} and Massimo Vergassola²¹ CNRS, INLN, 1361 Route des Lucioles, 06560 Valbonne, France.² CNRS, Observatoire de la Côte d'Azur, B.P. 4229, 06304 Nice Cedex 4, France.³ ISAC-CNR, Str. Prov. Lecce-Monteroni Km 1.200, I-73100 Lecce, Italy.⁴ INFN Dipartimento di Fisica, Università di Genova, Via Dodecaneso 33, I-16146 Genova, Italy.

(Dated: February 9, 2020)

Active and passive scalars transported by an incompressible two-dimensional conductive fluid are investigated. It is shown that a passive scalar displays a direct cascade towards the small scales while the active magnetic potential builds up large-scale structures in an inverse cascade process. Correlations between scalar input and particle trajectories are found to be responsible for those dramatic differences as well as for the behavior of dissipative anomalies.

PACS numbers: 47.27.-i

The transport of scalar fields by turbulent flows is a common physical phenomenon. In many situations, the dynamics of the advecting velocity field depends on the transported field, which is then dubbed active. That is, for instance, the case of temperature, which affects the velocity dynamics via buoyancy forces. Conversely, situations where the flow is not influenced by the scalar, e.g. for the concentration of a dilute tracer, are referred to as passive. Progress has been recently made for the passive case (see Ref. [1] and references therein). These studies put renewed emphasis on the known field-particle duality in the description of scalar transport. Long known concepts as intermittency, dissipative anomaly, direct and inverse cascades, usually defined in terms of field characteristics (the Eulerian description), can now be elegantly explained in terms of the statistical properties of particle trajectories (the Lagrangian description). In this Letter we address the problem of relating the Eulerian properties to the Lagrangian ones for active scalar transport.

The dynamics of an active field $a(\mathbf{x};t)$ advected by an incompressible flow $\mathbf{v}(\mathbf{x};t)$ is governed by the transport equation

$$\partial_t a + \mathbf{v} \cdot \nabla a = a + f: \quad (1)$$

The passive field $c(\mathbf{x};t)$ evolves in the same flow according to

$$\partial_t c + \mathbf{v} \cdot \nabla c = c + f: \quad (2)$$

The two scalars have the same diffusion coefficient while f_a and f_c are independent realizations of the same random forcing, with characteristic lengthscale l_f . The difference between the evolution of active and passive scalar resides in their relationship with the flow \mathbf{v} : the active field enters the velocity dynamics whereas the passive one does not. Here the evolution equation for \mathbf{v} is

$$\partial_t \mathbf{v} + \mathbf{v} \cdot \nabla \mathbf{v} = \nabla p - \nabla a + \nu \nabla^2 \mathbf{v}: \quad (3)$$

Eqs. (1) and (3) are the two-dimensional magnetohydrodynamics equations (see, e.g., Ref. [2]), with the following

glossary: a is the scalar magnetic potential; the magnetic field is $\mathbf{b} = (\partial_x a; \partial_y a)$; the coupling term ∇a is the Lorentz force $(\nabla \times \mathbf{b})$; the solenoidality condition $\nabla \cdot \mathbf{v} = 0$ is ensured by the pressure term ∇p and ν is the kinematic viscosity.

Besides its physical relevance, this example of active scalar is particularly interesting because of the conspicuous differences with respect to its passive counterpart. Namely, whilst a undergoes an inverse cascade process, i.e. it forms structures at increasingly larger scales, c cascades downscale (see Fig. 1) [2]. As a consequence, the dissipation of active scalar fluctuations by molecular diffusivity $\epsilon_a = \int |\nabla a|^2$ is vanishingly small in the limit $l_f \rightarrow 0$: no dissipative anomaly for the field a . Since the scalar variance is injected at a constant rate F_0 by the source f_a , we have that $\epsilon_a(t) = \frac{1}{2} \int |\nabla a|^2 dx$ increases linearly in time as $\frac{1}{2} F_0 t$. On the contrary, passive scalar dissipation $\epsilon_c = \int |\nabla c|^2$ equals the input $\frac{1}{2} F_0$ and holds c in a statistically stationary state (see Fig. 1).

Before discussing the Lagrangian interpretation of these results, let us present in some detail the outcome of our simulations from the Eulerian viewpoint. The probability distribution of a is Gaussian, with zero mean and variance $F_0 t$ (see Ref. [3], Fig. 5). This is a straightforward consequence of the vanishing of active scalar dissipation. Indeed, by averaging over the forcing statistics one obtains: $\partial_t \langle a^{2n} \rangle = n(2n-1) F_0 \langle a^{2n-2} \rangle$ (odd moments vanish by symmetry). The solutions are the moments of a Gaussian distribution: $\langle a^{2n} \rangle = (2n-1)!! (F_0 t)^n$. This may be contrasted with the single-point probability density function (pdf) of c which is stationary and supergaussian (see Ref. [3], Fig. 5), as it generically happens for a passive field sustained by a Gaussian forcing in a rough flow. Despite the growth of $\langle a^2 \rangle$, the increments of active scalar $\delta a = a(\mathbf{x} + \mathbf{r}; t) - a(\mathbf{x}; t)$ eventually reach a stationary state. In Fig. 2(a) we show the scale dependence of δa . At scales $r < l_f$ the active field is smooth, $\delta a \propto r$, in agreement with dimensional expectations (see e.g. [2, 4]). Above the injection lengthscale a scaling $\delta a \propto r^{1/2}$ emerges, corresponding to a spec-

trum $E_a(k) \sim k^{-2}$ for $k < k_f$ (see Ref. [3], Fig. 8). This result is dimensionally compatible with the observed scaling $\delta v = [v(x+r;t) - v(x;t)] \sim r^0$ for $r > l_f$ (see Fig. 2(b)), and the Yaglom relation $\delta v \sim (r a)^{2/3} F_0 r$. It is worth remarking that the discernibly different relation $\delta a \sim r^{2/3}$ for $r > l_f$, or $E_a(k) \sim k^{-7/3}$ for $k < k_f$ was also proposed [2, 4, 5]. However, the argument leading to that prediction rests on the assumption of locality for velocity increments, a hypothesis clearly incompatible with the observed velocity spectrum shallower than k^{-1} for $k < k_f$ (see Ref. [3], Fig. 6). As for the scaling of velocity increments below the forcing lengthscale, it is a much debated issue [6, 7]. Current opinions are divided between the Kolmogorov scaling $\delta v \sim r^{1/3}$, and the Iroshnikov-Kraichnan $\delta v \sim r^{1/2}$. Our data do not allow to discriminate between those two predictions. As shown in Fig. 2(c), the analysis of the scalar difference pdf's at various separations $r > l_f$ reveals that the active field is self-similar. The pdf of active scalar increments is subgaussian (see Fig. 2(d)), whereas passive scalar dif-

ferences in the same range show a supergaussian pdf (see Ref. [3], Fig. 7).

We now revert to the main purpose of this Letter, that is to investigate the statistical properties of active and passive scalar in the Lagrangian setting. The fundamental property which we will exploit in the following is that the equations (1) and (2) can be formally solved in terms of particle propagators. Let $X(s)$ be the trajectory of a fluid particle transported by the flow v and subject to a molecular diffusivity D , landing at point x at time t . The particle moves according to the stochastic differential equation $dX(s) = v(X(s);s)ds + \sqrt{2D} dB(s)$, where $B(s)$ is a two-dimensional brownian motion. Denoting by $p(y;s|x;t)$ the probability density of finding a particle at the point y at time $s < t$, we can write the solution of (1) and (2) as

$$a(x;t) = \int_0^t ds \int dy f_a(y;s) p(y;s|x;t); \quad (4)$$

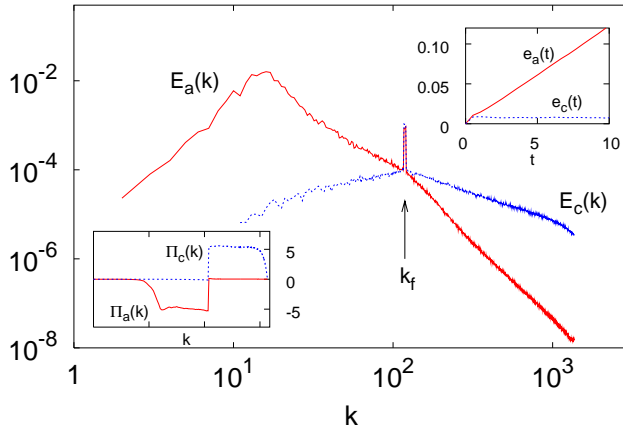


FIG. 1: Power spectra of active and passive scalar variances $E_a(k) = \langle k^2 \hat{a}(k;t)^2 \rangle$ and $E_c(k) = \langle k^2 \hat{c}(k;t)^2 \rangle$. The fluctuations of a injected at the forcing wavelength k_f flow towards smaller wavenumbers, whereas fluctuations of c cascade to larger ones. As a consequence, $E_a(k) > E_c(k)$ for $k < k_f$ and viceversa. In the lower left corner, the fluxes of scalar variance $\Pi_{a,c}$ out of wavenumber k . Negative values indicate an inverse cascade. In the upper right corner, the total scalar variance $e_{a,c}(t) = \int E_{a,c}(k;t) dk$. The active variance $e_a(t)$ grows linearly in time whereas $e_c(t)$ fluctuates around a finite value (see text). The rate of active to passive scalar dissipation is $\alpha = \epsilon / \epsilon_0 \approx 0.005$. The data result from the numerical integration of eqs. (1–3) by a dealiased pseudo-spectral parallel code, on a doubly periodic box of size 2π and resolution 4096^2 . The forcing terms f_a and f_c are homogeneous independent Gaussian processes with zero mean and correlation $\langle \hat{f}_i(k;t) \hat{f}_j(k';t') \rangle = \delta_{ij} \delta(k+k') \delta(t-t') F_0 = (2\pi k_f)^{-1} \delta(k+k') \delta(t-t')$ where $i,j = a,c$. The coefficients α and ϵ_0 are chosen to obtain a dissipative lengthscale of the order of the smallest resolved scales. All fields are set to zero at $t = 0$, and time is defined in units of eddy-turnover time $\tau = l_f / v_{rms}$ where $l_f = 2\pi / k_f$.

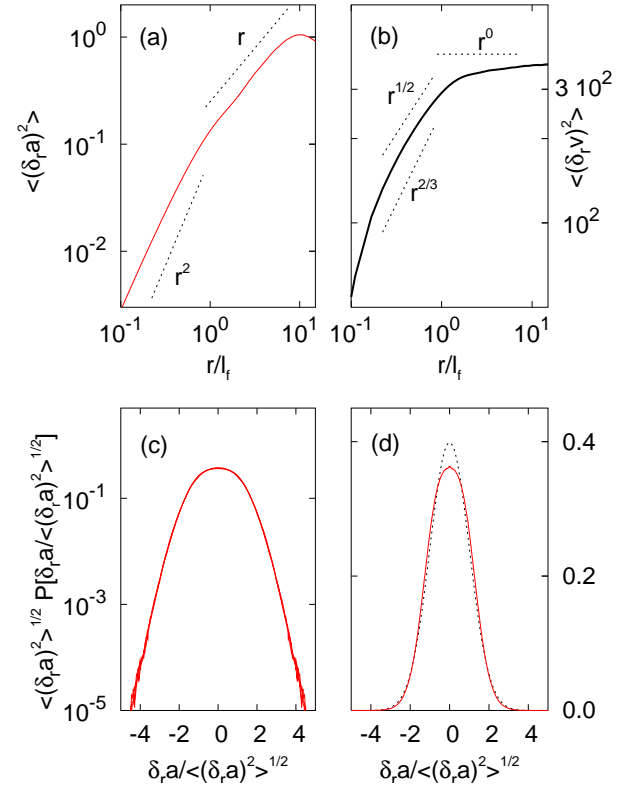


FIG. 2: (a) Scaling of active scalar increments δa . Here the symbol $\langle \cdot \rangle$ denotes spatial averaging over a single snapshot of the field. (b) Scaling of velocity increments δv . (c) Probability density functions of δa for $r = 2l_f; 3l_f; 4l_f$, rescaled by their standard deviation. The curves overlap almost perfectly, indicating self-similarity. (d) Rescaled probability density function of δa for $r = 3l_f$, now in linear scale, to emphasize the deviation from a Gaussian (dashed line). The kurtosis is 2.76, significantly smaller than the Gaussian value 3.

$$c(\mathbf{x};t) = \int_0^t ds \int d\mathbf{y} f_c(\mathbf{y};s) p(\mathbf{y};s|\mathbf{x};t) : \quad (5)$$

More compactly, $a(\mathbf{x};t) = \langle \int_0^t f_a(\mathbf{X}(s);s) ds \rangle_{\mathbf{x}}$, where $\langle \cdot \rangle_{\mathbf{x}}$ denotes the average over particle trajectories. A unique propagator p appears in both equations, since the velocity field in (1) and (2) is the same. The simple interpretation of eqs. (4) and (5) is that the value of the scalar field at $(\mathbf{x};t)$ is given by the superposition of the input along all trajectories eventually converging at that point and time. The different behavior between the active and the passive field is due to the correlations between the propagator p and the forcing f_a . Indeed, via the coupling term in eq. (3), f_a affects the velocity field and consequently the evolution of the propagator p . To further clarify the relationship between Lagrangian trajectories and active field forcing, it is necessary to investigate the evolution of the particle propagator. At first glance, this would seem a difficult task since p evolves backward in

time, according to the Kolmogorov equation

$$\partial_s p + \mathbf{v}(\mathbf{y}) \cdot \nabla_{\mathbf{y}} p = 0 : \quad (6)$$

The "initial" condition $p(\mathbf{y};t|\mathbf{x};t) = \delta(\mathbf{y} - \mathbf{x})$ is set at the final time t . Contrary to an usual forward integration, where \mathbf{v} and p can be advanced in parallel, a brute force backward integration would require the storage of velocity configurations for the whole lapse of integration. Times and resolutions involved in our simulations make that solution quite unfeasible. In fact, we devised a recursive algorithm [8] to integrate numerically eqs. (1), (3), and (6) with the same memory requirements and just three times the CPU time involved in the simple forward integration of eqs. (1) and (3) (for details see the Appendix in Ref. [3]). A typical evolution of the propagator is shown in the central column of Fig. 3. We can now reconstruct the time sequence of the forcing contributions $a_{a;c}(s) = \int d\mathbf{y} f_{a;c}(\mathbf{y};s) p(\mathbf{y};s|\mathbf{x};t)$ which, integrated over s , gives the amplitude of the scalar fields according to (4) and (5). As shown in Fig. 4, the time series of $a(s)$ and $c(s)$ are markedly different. In the active scalar case the sequence is strongly skewed towards positive values at all times. This signals that the trajectories preferentially select regions where f_a has a positive sign, summing up forcing contributions to generate a typical variance of a of the order $F_0 t$. Conversely, f_c can be positive or negative with equal probability on distant trajectories, and the time integral in eq. (5) averages out to zero for $j \gg t_j$ ($t_j = 1/\nu_{\text{rms}}$ is the eddy-turnover time). Therefore, typically $c^2 \ll F_0$. The cumulative effect of the correlation between forcing and propagator is even more evident from the relation $\int_0^t a(s^0) ds^0 = \int d\mathbf{y} a(\mathbf{y};s) p(\mathbf{y};s|\mathbf{x};t)$

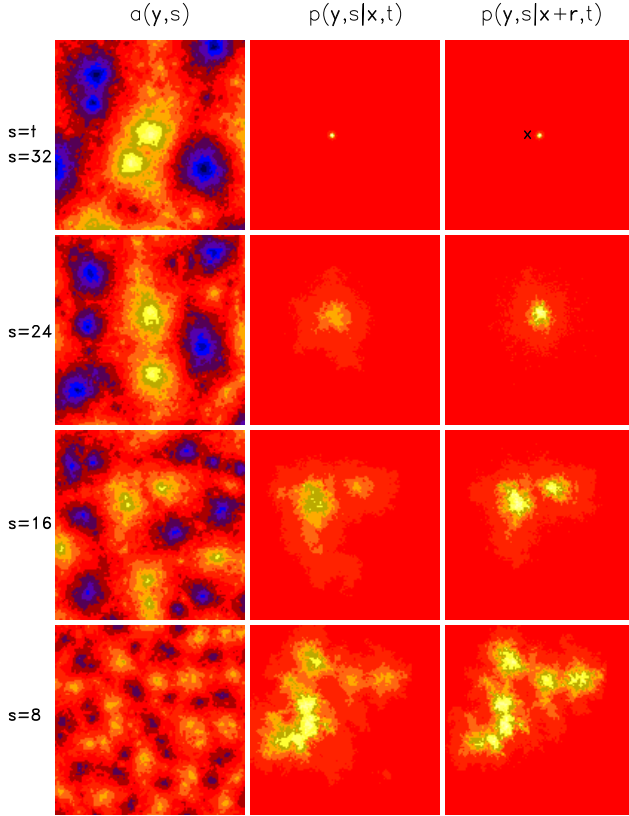


FIG. 3: First column, from bottom to top: time evolution of the active scalar field resulting from the numerical integration of eqs. (1) and (3). Second column, from top to bottom: backward evolution of the particle propagator according to eq. (6). Third column, from top to bottom: as in the second column, but with a propagator initialized at $\mathbf{x} + \mathbf{r}$ at time t , with $r = 2.5 l_f$. As a term of comparison, the point \mathbf{x} is marked by a cross. For a discussion, see text.

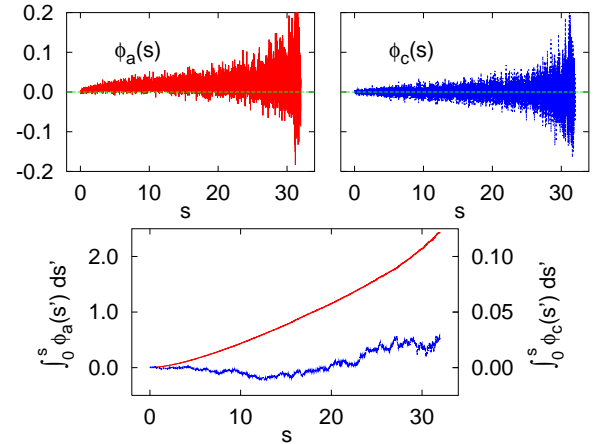


FIG. 4: Top: $a_{a;c}(s) = \int d\mathbf{y} f_{a;c}(\mathbf{y};s) p(\mathbf{y};s|\mathbf{x};t)$. The two graphs have the same scale on the vertical axis. Here, $t = 32$. Bottom: time integrals $\int_0^t a(s^0) ds^0$ (upper curve) and $\int_0^t c(s^0) ds^0$ (lower curve). Note the different scale on the vertical axis. Recall that $\int_0^t a(s^0) ds^0 = a(\mathbf{x};t)$ (and similarly for c).

derived from (1) and (6). As shown in Fig. 4, the growth of the scalar variance is thus related to a strong spatial correlation between the propagator and the active field. That is further evidenced by comparing the first and the second column of Fig. 3: the distribution of particles closely follows the distribution of like-sign active scalar (for an animation, see [3]). This amounts to say that large-scale scalar structures are built out of smaller ones which "coalesce" together [5].

As remarked previously, the absence of dissipative anomaly is closely related to the onset of an inverse cascade. Let us now discuss this issue from a Lagrangian viewpoint and consider the squared active field a^2 . On one hand, it can be written as the square of (4). On the other hand, one can multiply (1) by $2a$ to obtain the equation $\partial_t a^2 + \nabla \cdot \mathbf{r} a^2 = a^2 + 2af_a - 2a$ and solve it for $a = 0$ in terms of particle trajectories. The comparison of the two previous expressions yields

$$\int_0^t \int_{\mathbf{r}} \int_{\mathbf{s}} \int_{\mathbf{s}^0} \frac{ds}{ds^0} f_a(\mathbf{y};s) f_a(\mathbf{y}^0;s^0) p(\mathbf{y};s;\mathbf{x};t) p(\mathbf{y}^0;s^0;\mathbf{x};t) = \int_0^t \int_{\mathbf{r}} \int_{\mathbf{s}} \int_{\mathbf{s}^0} \frac{ds}{ds^0} f_a(\mathbf{y};s) f_a(\mathbf{y}^0;s^0) p(\mathbf{y}^0;s^0;\mathbf{y};s;\mathbf{x};t); \quad (7)$$

where $p(\mathbf{y}^0;s^0;\mathbf{y};s;\mathbf{x};t) = p(\mathbf{y};s;\mathbf{x};t)p(\mathbf{y}^0;s^0;\mathbf{y};s)$ denotes the probability that a trajectory ending in $(\mathbf{x};t)$ were in $(\mathbf{y};s)$ and $(\mathbf{y}^0;s^0)$. Integration over \mathbf{y} and \mathbf{y}^0 is implied. In a more compact notation, eq. (7) can be recast as $\int_0^t \int_{\mathbf{r}} f_a(\mathbf{x}(s);s) ds \int_0^t \int_{\mathbf{r}} f_a(\mathbf{x}(s^0);s^0) ds^0 = \int_0^t \int_{\mathbf{r}} f_a(\mathbf{x}(s);s) ds \int_0^t \int_{\mathbf{r}} f_a(\mathbf{x}(s^0);s^0) ds^0$, leading to the conclusion that $\int_0^t \int_{\mathbf{r}} f_a(\mathbf{x}(s);s) ds$ is a non-random variable over the ensemble of trajectories. This result has a simple interpretation: the absence of dissipative anomaly is equivalent to the property that each trajectory ending in $(\mathbf{x};t)$ contributes exactly the same amount to build up $a(\mathbf{x};t)$. A straightforward consequence is that the single-point pdf of a is Gaussian, consistently with the Eulerian argument given above. It is interesting to recall that the lack of dissipative anomaly has been previously related to Lagrangian properties in the context of passive scalar transport by a compressible flow [9]. In that case, the ensemble of trajectories collapses onto a unique path, fulfilling in the simplest way the condition (7). Here, even though the trajectories do not collapse, the constraint (7) is satisfied due to the subtle correlation between forcing and trajectories peculiar to the active case.

As to the two-point statistics, active scalar differences are obtained by subtracting the contribution of trajectories ending in \mathbf{x} to the contribution of those ending in $\mathbf{x} + \mathbf{r}$. Therefore, τ_a is the difference of two Gaussian

variables, which are however strongly correlated, as shown in Fig. 3. This correlation leads to strong cancellations resulting in the time stationarity of the statistics of τ_a , and in its observed subgaussian behavior. It is interesting to point out that universality of active scalar statistics is due to the self-averaging property (7), that is to a different mechanism from the one at work in the passive case.

We conclude with a discussion of the following open issue. It is known that passive field correlation functions are controlled by the asymptotically dominant terms in particle propagators (see, e.g., Ref. [1]). Is this also true for active scalars? The correlations between propagator and input in (4) suggest this be not the general rule. For some specific systems, those correlations might however be such that the asymptotics of the propagator will still stand out at large times [10, 11]. Clarifying the dynamical conditions controlling this phenomenon will be the subject of future work.

We acknowledge useful discussions with A. Noullez and I. Procaccia. This work has been supported by the EU under the contract HPRN-CT-2000-00162, and by Indo-French Center for the Promotion of Advanced Research (IFCPA R2404-2). AM has been partially supported by Con2001 (prot.2001023842). Numerical simulations have been performed at IDRIS (project 021226) and at CINECA (INFM parallel computing initiative).

-
- [1] G. Falkovich, K. Gawedzki, and M. Vergassola, *Rev. Mod. Phys.* 73, 913 (2001).
 - [2] D. Biskamp, *Nonlinear magnetohydrodynamics*, Cambridge University Press, Cambridge, UK (1993).
 - [3] <http://www.obs-nice.fr/cencini>
 - [4] A. Pouquet, *J. Fluid Mech.* 88, 1 (1978).
 - [5] D. Biskamp, and U. Brenner, *Phys. Rev. Lett.* 72, 3819 (1994).
 - [6] D. Biskamp, and E. Schwarz, *Phys. Plasmas* 8, 3282 (2001).
 - [7] H. Politano, A. Pouquet, and V. Carbone, *Europhys. Lett.* 43, 516 (1998).
 - [8] We are grateful to A. Noullez for illuminating suggestions on the algorithm.
 - [9] K. Gawedzki, and M. Vergassola, *Physica D*, 138, 63 (2000).
 - [10] E. S. C. Ching, Y. Cohen, T. Gilbert and I. Procaccia, *Europhys. Lett.* (2002) in press, see also nlin.CD/0111030.
 - [11] A. Celani, T. Matsumoto, A. Mazzino and M. Vergassola, *Phys. Rev. Lett.*, 88, 054503 (2002).